

Ab initio Study of Graphene on SiC

Alexander Mattausch* and Oleg Pankratov

Theoretische Festkörperphysik, Universität Erlangen-Nürnberg, Staudtstr. 7, 91058 Erlangen, Germany

(Dated: February 17, 2014)

Employing density-functional calculations we study single and double graphene layers on Si- and C-terminated 1×1 -6H-SiC surfaces. We show that, in contrast to earlier assumptions, the first carbon layer is covalently bonded to the substrate, and cannot be responsible for the graphene-type electronic spectrum observed experimentally. The characteristic spectrum of free-standing graphene appears with the second carbon layer, which exhibits a weak van der Waals bonding to the underlying structure. For Si-terminated substrate, the interface is metallic, whereas on C-face it is semiconducting or semimetallic for single or double graphene coverage, respectively.

PACS numbers: 68.35.Ct, 68.47.Fg, 73.20.-r

The last years have witnessed an explosion of interest in the prospect of graphene-based nanometer-scale electronics [1, 2, 3, 4]. Graphene, a single hexagonally ordered layer of carbon atoms, has a unique electronic band structure with the conic “Dirac points” at two inequivalent corners of the two-dimensional Brillouin zone. The electron mobility may be very high and lateral patterning with standard lithography methods allows device fabrication [1]. Two ways of obtaining graphene samples have been used up to now. In the first “mechanical” method, the carbon monolayers are mechanically split off the bulk graphite crystals and deposited onto a SiO_2/Si substrate [4]. This way an almost “free-standing” graphene is produced, since the carbon monolayer is practically not coupled to the substrate. The second method uses epitaxial growth of graphite on single-crystal silicon carbide (SiC). The ultrathin graphite layer is formed by vacuum graphitization due to Si depletion of the SiC surface [5]. This method has apparent technological advantages over the “mechanical” method, however it does not guarantee that an ultrathin graphite (or graphene) layer is electronically isolated from the substrate. Moreover, one expects a covalent coupling between both which may strongly modify the electronic properties of the graphene overlayer. Yet, experiments show that the transport properties of the interface are dominated by a single epitaxial graphene layer [1, 2]. Most surprisingly, the electronic spectrum seems not to be affected much by the substrate. As in free-standing graphene one observes the “Dirac points” with the linear dispersion relation around them. The electron dynamics is governed by a Dirac-Weyl Hamiltonian with the Fermi velocity of graphene replacing the speed of light. This leads to an unusual sequence of Landau levels in a magnetic field and hence to peculiar features in the quantum Hall effect [1, 4].

The growth of high-quality graphene layers on both Si-terminated or C-terminated $\text{SiC}\{0001\}$ surfaces occurs in vacuum at annealing temperatures above 1400°C . The geometric structure of the interface is unclear. Forbeaux *et al.* [5] proposed that on the Si-face the graphite

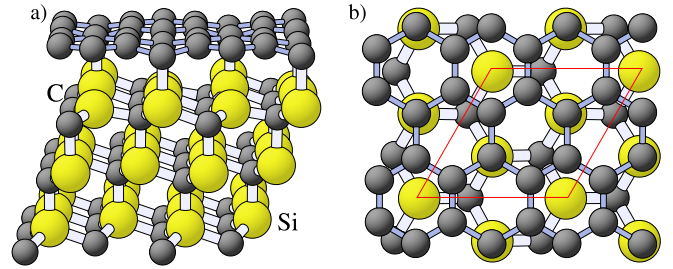


FIG. 1: (Color online) Side view (a) and top view (b) of a graphene layer on the $\text{SiC}(0001)$ surface. The $\sqrt{3} \times \sqrt{3}R30^\circ$ surface unit cell is highlighted.

layer is loosely bound by van der Waals-forces to the $\sqrt{3} \times \sqrt{3}R30^\circ$ -reconstructed substrate. On the contrary, combining STM and LEED data with DFT calculations Chen *et al.* [6] came to the conclusion that the graphite sheet is formed on a complex 6×6 -structure, from which originates the observed $6\sqrt{3} \times 6\sqrt{3}R30^\circ$ reconstruction that precedes the graphite formation. On the C-terminated $\text{SiC}(000\bar{1})$ face, graphite growth on top of a 2×2 reconstruction was reported [5, 7]. Berger *et al.* [1, 2] observed the formation of large high-quality graphene islands on top of a 1×1 C-terminated SiC substrate with a $\sqrt{3} \times \sqrt{3}R30^\circ$ interface reconstruction.

In this work we employ an *ab initio* density-functional theory approach to study the bonding and electronic structure of graphene on SiC. We find that a strong covalent bonding of the first carbon layer to the substrate removes the graphene-type electronic features from the energy region around the Fermi level. However, these features reappear with the second carbon layer. We also compare the electronic properties of graphene on Si- and C-terminated surfaces.

Our calculations were performed with the density-functional theory program package VASP [8, 9, 10, 11] in the local spin density approximation (LSDA). Projector augmented wave (PAW) pseudopotentials [12] were used. A special $7 \times 7 \times 1$ \mathbf{k} -point sampling was applied for the Brillouin-zone integration. The plane wave basis set was

restricted by a cut-off energy of 400 eV. We have chosen a 6H-SiC polytype, which is most often used in experimental studies. The supercell was constructed of 6 bi-layers of SiC in the S3-structure [13], one or two carbon monolayers and a vacuum interval needed to separate the slabs. The vacuum separation varied, depending on the carbon coverage, between 10 to 15 Å. The graphene layer was placed on top of the unreconstructed 6H-SiC substrate such that the structure had a lateral $\sqrt{3} \times \sqrt{3}R30^\circ$ elementary cell (Fig. 1a). Due to the lattice mismatch of 8% between SiC and graphite, this requires stretching the graphene layer. We verified that for the free-standing graphene layer the stretch reduces the total bandwidth from 19.1 eV to 17.3 eV but does not affect the electronic spectrum close to the Fermi energy. The elastic energy is 0.8 eV per graphene unit cell.

The interface unit cell (cf. Fig. 1b) contains three surface atoms of the substrate and four elementary unit cells of graphene. The dangling bonds of the substrate atoms at the corners of the unit cell are unsaturated, while the other surface atoms bind to two carbon atoms of the hexagonal graphene ring. In case of the Si-terminated SiC(0001) surface, we find that the graphene layer is separated by 2.58 Å from the SiC substrate. The carbon atoms covalently bonded to the substrate relax towards the SiC surface, such that the bond length is 2.0 Å. This is only slightly longer than the bond length 1.87 Å in SiC. The graphene bonding releases 0.72 eV per graphene unit cell. For the C-terminated SiC(000 $\bar{1}$) face, the graphene layer is somewhat closer (2.44 Å) to the substrate and the bond length between the bonding carbon atoms reduces to 1.87 Å. The energy gain is 0.60 eV per graphene unit cell. On both interfaces, the bonding atom of the substrate relaxes outwards, whereas the partner graphene atom moves towards the substrate. The bonding energies are quite close but somewhat smaller than the elastic deformation energy of the graphene layer. However, the latter can be drastically lessened by defects which result from the lattice mismatch.

For a second graphene layer placed in the graphite-type AB stacking, we find a weak bonding at a distance of 3.3 Å, very close to the bulk graphite value 3.35 Å. This conforms to the fact that LSDA, despite the lack of long-range non-local correlations, produces reasonable interlayer distances in van der Waals crystals like graphite [14, 15] or *h*-BN [16]. As shown by Marini *et al.* [16], a delicate error cancellation between exchange and correlation underlies this apparent performance of the LSDA. The semilocal GGA, which violates this balance, fails to generate the interplanar bonding in both graphite [15] and *h*-BN [16], while producing a band structure identical to LSDA [15]. It is thus natural to assume that in our situation the bonding between the graphene layers is the same as in bulk graphite with the same interplanar distance. To reduce the calculational cost, we fixed the interplanar distance at this value.

The first graphene layer, which is covalently bonded to the substrate, thus serves as a buffer separating the SiC crystal and the van der Waals bonded second graphene sheet. Most probably, the $6\sqrt{3} \times 6\sqrt{3}R30^\circ$ reconstructed carbon-rich Si-terminated surface observed as a precursor of graphitization is a natural realization of this buffer layer in the epitaxial process. The $6\sqrt{3} \times 6\sqrt{3}$ structure is practically commensurate with graphene since 13 times the graphene lattice constant almost precisely fits $6\sqrt{3}$ times the SiC lattice parameter. In any case, there is no stress in the second carbon layer. Even placed on a strongly stretched buffer layer, the upper layer relaxes to its natural lattice constant due to the weak interlayer interaction. For the C-face Berger *et al.* [1] found graphene formation on a 1×1 substrate with a $\sqrt{3} \times \sqrt{3}$ interface unit cell. This structure is the same as we used in our calculations.

Figs. 2a and 2b show the electronic energy spectrum of a single graphene layer on the two SiC surfaces. The shaded regions are the projected conduction and valence energy bands of SiC. The Kohn-Sham energy gap of 1.98 eV is smaller than the optical band gap (3.02 eV) of the bulk 6H-SiC, which is a common consequence of LSDA. The covalent bonding drastically changes the graphene electron spectrum at the Fermi energy. The “Dirac cones” are merged into the valence band, whereas the upper graphene bands overlap with the SiC conduction band. Hence a wide energy gap emerges in the graphene spectrum. A similar gap opening due to hydrogen absorption on a single graphene sheet was predicted in Ref. 17. The weakly dispersive interface states visible in Figs. 2a and 2b result from the interaction of the graphene layer with the three dangling orbitals of the substrate. Two of them make covalent bonds, while the third one in the center of the graphene ring remains unsaturated (cf. Fig. 1b). A projection analysis of the wave functions reveals that the gap states close to the Fermi energy originate from the remaining dangling bonds of the substrate. On the Si-face we find a half-filled metallic state, whereas on the C-face the interface state is split into a singly occupied (spin polarized) and an empty state, making the interface insulating. In contrast, on both clean SiC surfaces LSDA predicts a substantial splitting of the surface states (0.86 eV for SiC(0001) and 0.45 eV for SiC(000 $\bar{1}$), see Table I). Actually, the gap separating a singly occupied and an empty state is larger due to the Hubbard repulsion of the electrons (about 2 eV for the $\sqrt{3} \times \sqrt{3}R30^\circ$ reconstructed surface [18, 19]), but already LSDA correctly reproduces the insulating character of both surfaces.

The reason for the striking difference between the two graphene-covered surfaces becomes clear if one compares the planar localization of the two gap states. As seen in Fig. 3a for the Si-face the interface state electron density is strongly delocalized. As the projection analysis shows, this results from the hybridization with the graphene-

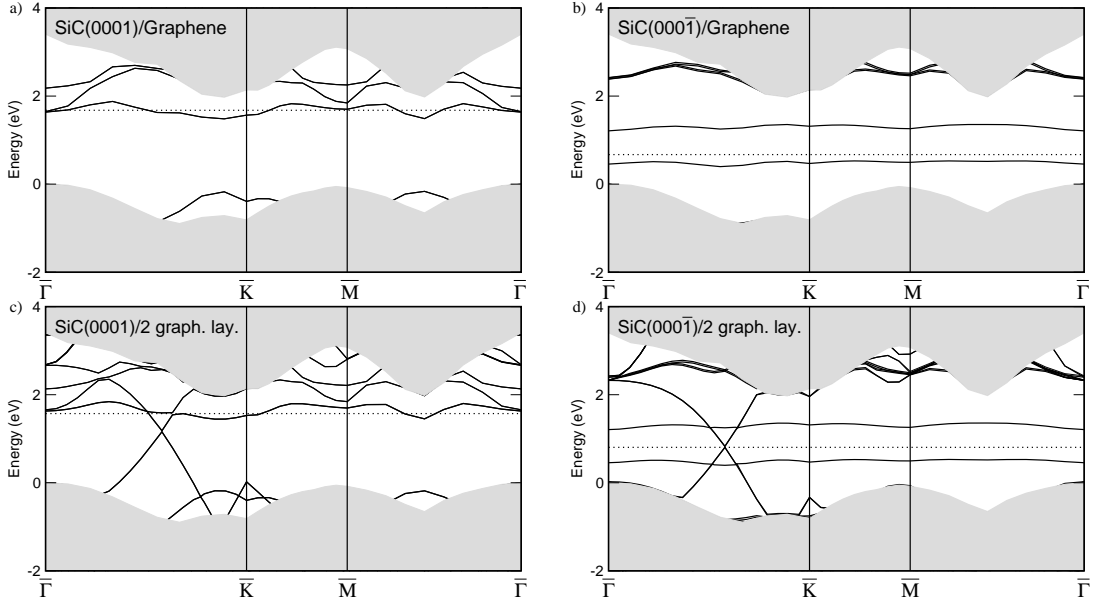


FIG. 2: Energy spectrum of the interface states of a) the SiC(0001)/graphene interface, b) the SiC(0001̄)/graphene interface, c) SiC(0001) with two layers of graphene and d) SiC(0001̄) with two layers of graphene. The Fermi energy is indicated by the dashed line. \bar{K} and \bar{M} are the high-symmetry points of the surface Brillouin zone of the $\sqrt{3} \times \sqrt{3}R30^\circ$ surface unit cell.

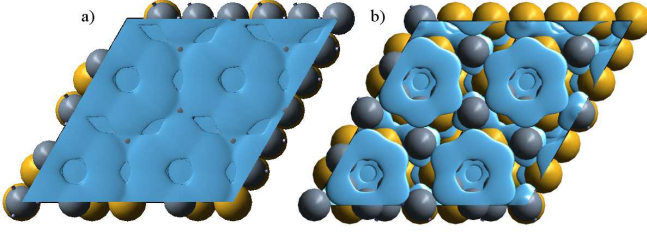


FIG. 3: (Color online) Charge density of the interface states at the Fermi energy for a single graphene layer on a) SiC(0001) and b) SiC(0001̄).

induced electron states overlapping with the conduction band (see Fig. 2a). Given the delocalized nature of the interface state we expect the influence of Hubbard correlations to be small. In contrast, at the C-terminated substrate the electron state retains its localized character, although it is smeared over a carbon ring just above the unsaturated C-dangling bond. The localization favors the spin polarization and thus the splitting of the gap state, whereas the interface state at the Si-face remains spin-degenerate. In the former case, Hubbard correlations may lead to a further splitting of the interface state.

Figures 2c and 2d show that the second carbon layer indeed possesses an electronic structure similar to free-standing graphene. The characteristic conic point appears on the $\bar{\Gamma} - \bar{K}$ line (note that since the Brillouin zone corresponds to the $\sqrt{3} \times \sqrt{3}R30^\circ$ unit cell, the conic

point is not located at the \bar{K} -point). The interface states of the buffer layer remain practically unchanged since the interaction of the carbon layers is very small. The metallic interface state on the Si-terminated substrate pins the Fermi level just above the conic point, making the second graphene layer *n*-doped. On C-terminated substrate the Fermi level runs exactly through the conic point. Hence the interface is semimetallic just as for free-standing graphene. Indeed, for a graphene-covered C-face Berger *et al.* [1] found that the thin graphite layers possess electronic properties of free-standing graphene.

The parameters of the electron states for the different interfaces are summarized in Table I. For clean unreconstructed surfaces we find work functions of 4.75 eV (Si-terminated surface) and 5.75 eV (C-terminated surface). The former value is practically the same as the work function of the reconstructed SiC(0001) [20]. The first graphene layer reduces this value to 3.75 eV, which is 1.3 eV lower than the work function of free-standing graphene. The drastic reduction of the work function is caused by charge flow from graphene to the interface region, which induces a dipole layer. On the C-face the graphene overlayer also reduces the work function, but to a lesser extent such that it remains above the graphene value. Adding the second graphene layer makes the work function closer to that of graphene for both faces.

The Fermi level pinning close to the conduction band makes the graphitized Si-face especially suitable for Ohmic contacts on *n*-type SiC, because it guarantees a low Schottky barrier. Indeed, Lu *et al.* [21] find a very low resistance for thermally treated SiC contacts with

TABLE I: Parameters of the unreconstructed and graphene-covered SiC{0001} surfaces in eV: work function ϕ , positions of the occupied and the unoccupied surface and interface states above the valence band edge (E_o , E_u) and their corresponding bandwidths (B_o , B_u).

	Work function ϕ	E_o	B_o	E_u	B_u
SiC(0001) 1×1	4.75	$E_v + 0.92$	0.45	$E_v + 1.78$	0.53
SiC(0001)/Graphene	3.75	$E_v + 1.64$	0.35	—	—
SiC(0001)/2 Graphene	4.33	$E_v + 1.64$	0.40	—	—
SiC(000 $\bar{1}$) 1×1	5.75	$E_v + 0.05$	0.75	$E_v + 0.50$	0.45
SiC(000 $\bar{1}$)/Graphene	5.33	$E_v + 0.43$	0.13	$E_v + 1.19$	0.14
SiC(000 $\bar{1}$)/2 Graphene	5.31	$E_v + 0.44$	0.10	$E_v + 1.19$	0.15
Graphene (single layer)	5.11				

nickel and cobalt, while other metals, which form carbides and thereby remove the graphitic inclusions, were rectifying. Recently Seyller *et al.* measured the Schottky barrier between n -type 6H-SiC(0001) and graphite by photoelectron spectroscopy and found a low value of 0.3 eV [22]. On the contrary, the C-terminated face has the Fermi level close to the middle of the band gap and is semiconducting or semimetallic.

In conclusion, we investigated the interface between 1×1 - 6H-SiC{0001} surfaces and carbon layers employing *ab initio* density-functional theory. We find that graphene overlayers on SiC(0001) and SiC(000 $\bar{1}$) faces possess qualitatively different electronic structures. While the former is metallic, the latter has semiconducting properties. The conic points at the Fermi energy, which are specific for graphene, appear only with the second layer. The first carbon sheet is covalently bound to the substrate and plays the role of a transition region between a covalent SiC crystal and a van der Waals bonded stack of graphene layers.

This work was supported by Deutsche Forschungsgemeinschaft within the SiC Research Group. We are grateful to Valerio Olevano for communicating to us similar results on the SiC/graphene system [23] and fruitful discussions.

* Electronic address: Alexander.Mattausch@physik.uni-erlangen.de

- [1] C. Berger, Z. Song, X. Li, X. Wu, N. Brown, C. Naud, D. Mayou, T. Li, J. Hass, A. N. Marchenkov, et al., *Science* **312**, 1191 (2006).
- [2] J. Hass, C. A. Jeffrey, R. Feng, T. Li, X. Li, Z. Song, C. Berger, W. A. de Heer, P. N. First, and E. H. Conrad, *Appl. Phys. Lett.* **89**, 143106 (2006), cond-mat/0604206.
- [3] T. Seyller, K. V. Emtsev, K. Gao, F. Speck, L. Ley, A. Tadich, L. Broekmann, J. D. Riley, R. C. G. Leckey, O. Rader, et al., *Surf. Sci.* **600**, 3906 (2006).
- [4] Y. Zhang, Z. Jiang, J. P. Small, M. S. Purewal, Y.-W. Tan, M. Fazlollahi, J. D. Chudow, J. A. Jaszczak, H. L. Stormer, and P. Kim, *Phys. Rev. Lett.* **96**, 136806 (2006).
- [5] I. Forbeaux, J.-M. Themlin, and J.-M. Debever, *Phys. Rev. B* **58**, 16396 (1998).
- [6] W. Chen, H. Xu, L. Liu, X. Gao, D. Qi, G. Peng, S. C. Tan, Y. Feng, K. P. Loh, and A. T. S. Wee, *Surf. Sci.* **596**, 176 (2005).
- [7] I. Forbeaux, J.-M. Themlin, A. Charrier, F. Thibaudau, and J.-M. Debever, *Appl. Surf. Sci.* **162-163**, 406 (2000).
- [8] G. Kresse and J. Hafner, *Phys. Rev. B* **47**, 558 (1993).
- [9] G. Kresse, Ph.D. thesis, Technische Universität Wien, Austria (1993).
- [10] G. Kresse and J. Furthmüller, *Phys. Rev. B* **54**, 11169 (1996).
- [11] G. Kresse and J. Furthmüller, *Comput. Mat. Sci.* **6**, 15 (1996).
- [12] G. Kresse and D. Joubert, *Phys. Rev. B* **59**, 1758 (1999).
- [13] U. Starke, J. Schardt, J. Bernhardt, M. Franke, and K. Heinz, *Phys. Rev. Lett.* **82**, 2107 (1999).
- [14] J.-C. Charlier, X. Gonze, and J. P. Michenaud, *Carbon* **32**, 289 (1994).
- [15] N. Ooi, A. Rairkar, and J. B. Adams, *Carbon* **44**, 231 (2006).
- [16] A. Marini, P. García-González, and A. Rubio, *Phys. Rev. Lett.* **96**, 136404 (2006).
- [17] E. J. Duplock, M. Scheffler, and P. J. D. Lindan, *Phys. Rev. Lett.* **92**, 225502 (2004).
- [18] M. Rohlfing and J. Pollmann, *Phys. Rev. Lett.* **84**, 135 (2000).
- [19] V. I. Anisimov, A. E. Bedin, M. A. Korotin, G. Santoro, S. Scandolo, and E. Tosatti, *Phys. Rev. B* **61**, 1752 (2000).
- [20] M. Wiets, M. Weinelt, and T. Fauster, *Phys. Rev. B* **68**, 125321 (2003).
- [21] W. Lu, W. C. Mitchel, G. R. Landis, T. R. Crenshaw, and W. E. Collins, *J. Appl. Phys.* **93**, 5397 (2003).
- [22] T. Seyller, K. V. Emtsev, F. Speck, K.-Y. Gao, and L. Ley, *Appl. Phys. Lett.* **88**, 242103 (2006).
- [23] V. Olevano, private communication.